MINERALOGICAL MAGAZINE, JUNE 1983, VOL. 47, pp. 161-176

Crystallization of plagioclase, augite, and olivine in synthetic systems and in tholeiites

G. M. BIGGAR

Department of Geology, University of Edinburgh, West Mains Road, Edinburgh EH9 3JW

ABSTRACT. Experimental data from the system CaO-MgO-Na_2O-Al_2O_3-SiO_2 and from the system CaO-MgO-FeO-Al_2O_3-SiO_2 are used to show the nature of the changes in composition, with temperature and with pressure, of liquids in equilibrium with augite, plagioclase, and olivine as MgO in the system CaO-MgO-Al_2O_3-SiO_2 is partially replaced by FeO and as Na_2O replaces CaO. As differentiation of tholeiitic basalts proceeds, Fe/Mg increases, Na/Ca increases, and normative hypersthene increases and these effects alter the solubilities, and hence the proportions of augite, plagioclase, and olivine which co-precipitate. In particular olivine becomes more soluble (less is precipitated) as Fe/Mg increases; plagioclase becomes more soluble but augite less soluble as Na/(Na + Ca) increases; augite also becomes less soluble as normative hypersthene increases, and as pressure is reduced during ascent.

Experimental data from remelted ocean tholeiites encounter the same equilibrium and are presented and compared with the data from synthetic systems.

Some natural examples of daughter liquids related to parents by crystallization of augite, plagioclase, olivine, are combined with the experimental data and with some model calculations to demonstrate that only a very limited range of proportions of augite : plagioclase : olivine (approximately 30 : 50 : 15 to 20 : 60 : 20) produces daughter liquids which lie on the major element variation of the tholeiitic basalt series. Other proportions lead to daughter liquids which are not basalts. In the light of these restrictions, several recent publications are reinterpreted as examples of fractionation of augite, plagioclase, and olivine, rather than examples of partial melting. The recognition of the small effect that massive (50 to 83%) crystallization has on basaltic chemistry by contrast with the large effect that small accumulations of phenocrysts can have is particularly emphasized in this reinterpretation.

Comparisons and possible relationships are suggested between some low-K_2O, low-TiO_2 tholeiites; some calcic-, aphyric-, dykes of some tholeiitic provinces; some chilled margins of some layered intrusions; some basalts from Iceland, and some basalts from the ocean ridges.

THE aim of this paper is to understand phase equilibria involving augite, plagioclase, olivine, and liquid, in compositions in the system SiO_2-CaO-MgO-Al_2O_3 (sometimes with FeO or with Na_2O) and in tholeiitic magmas. The first section summarizes synthetic systems; the second section decribes experimental data for oceanic tholeiites and in the third, petrographic and chemical data from suites of rocks are plotted and compared with data from synthetic systems. Many natural trends can be interpreted in terms of crystallization of augite, plagioclase, and olivine, and particular emphasis is put on the proportions of these phases which precipitate during cooling of magmas to demonstrate that the proportions are nearly constant despite changes in the anorthite : albite ratio, in the MgO : FeO ratio, and in the total pressure. Later sections re-examine recent publications of oceanic basalt chemistry and show that chemical variations could as easily be due to crystal fractionation as to the alternative of partial melting, advocated by the authors of several of these publications.

Experimental data in the system CaO-MgO-FeO-Al_2O_3-SiO_2

Experimental data and projection techniques in the quaternary system CaO-MgO-Al_2O_3-SiO_2 have been adequately discussed by Cox *et al.* (1979, chaps. 8 and 9) and by Presnall *et al.* (1978, 1979). These data appear as curves in figs. 5 and 8. In the quinary system formed by the addition of Na_2O, data for the equivalent field boundaries have been published (Biggar and Humphries, 1981) and designated a_2, a_3, a_4, a_5, (at different anorthite to albite ratios) and these points appear in fig. 4B.

For the quinary system formed by adding FeO (strictly FeO plus Fe_2O_3) to CaO-MgO-Al_2O_3-SiO_2, many data reside in a thesis (Humphries, 1975) from which an extensive series of diagrams has been recently published (Humphries and Biggar, 1981). Representative figures (figs. 1A to C) give some temperatures and some compositions for the equilibria between augite, anorthite, olivine, and liquid and as examples of the use that can be made of this information, the compositions and temperatures from fig. 1A, designated a_6 at 1262 °C and g_6 at 1320 °C are used to sketch the likely

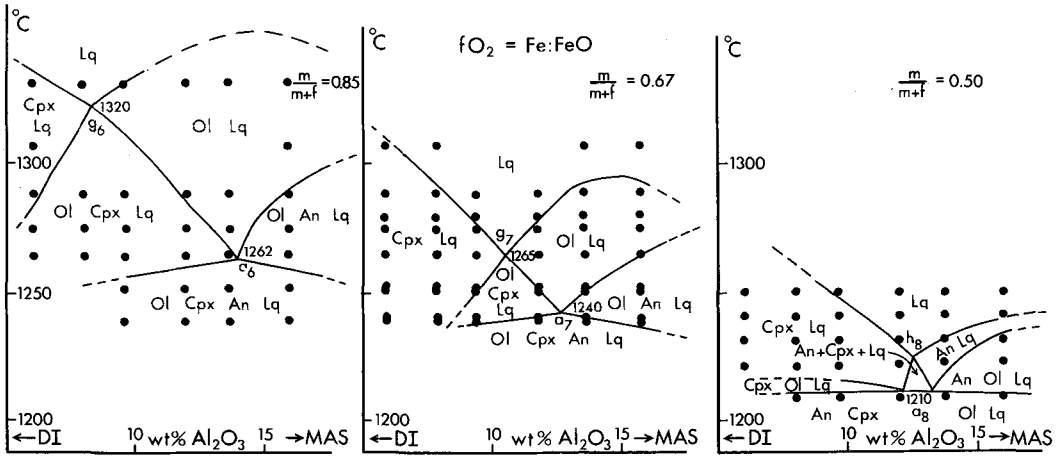

FIG. 1. Experimental data for parts of the join $Ca(Mg,Fe)Si_2O_6$-$(Mg,Fe)Al_2SiO_6$ at three values of the molar ratio Mg/(Mg+Fe) (0.85, 0.67, and 0.50) plotted with FeO recalculated as its molar equivalent of MgO and then plotted in wt.% (O'Hara, 1976, p. 103 et seq.) All data were obtained with f_{O_2} controlled at the iron–wüstite buffer. Temperatures at which fields meet are designated a_6, a_7, a_8, and g_6, g_7, and h_8 and are used in the construction of figs. 2A and B.

positions of the augite–olivine, and the anorthite–augite–olivine boundaries, as shown in fig. 2A. A similar treatment of compositions and temperatures in figs. 1B and C, along with information from Biggar and Humphries (1981, fig. 4A) for the quaternary (iron-free) system leads to the construction of fig. 2B, which shows the changes in composition and temperature of the field boundaries, as MgO, in the system CaO–MgO–Al_2O_3–SiO_2, is partially replaced by FeO. These figures demonstrate that as FeO replaces MgO both the anorthite and augite crystallization volumes increase while that of olivine diminishes. Olivine is no longer a liquidus phase in fig. 1C and this same feature shows in fig. 2B by the fact that when molar Mg/(Mg+Fe) = 0.5 the olivine field does not reach the line DI–K on which the compositions lie. Temperatures of equivalent points decline as FeO replaces MgO.

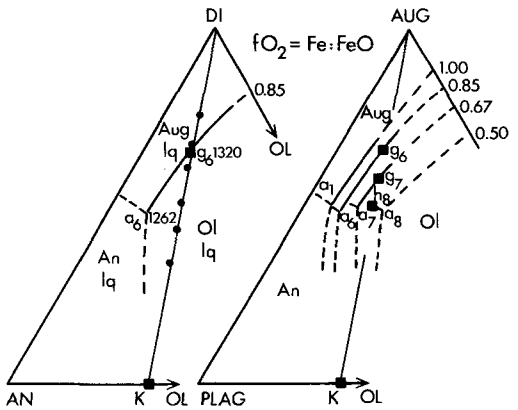

FIG. 2A (*left*). The plane anorthite–augite–olivine (in which the Mg/(Mg+Fe) ratio is 0.85) showing the experimentally investigated compositions (the same compositions as in fig. 1A) and a sketch of the field boundaries, based on points a_6 and g_6. Experimental compositions lie on the line DI–K (K has a molar composition $CaO{\cdot}Al_2O_3{\cdot}2(Mg,Fe)0.3SiO_2$—see also Biggar and Humphries, 1981). FIG. 2B (*right*). Similar to fig 2A, but superimposing information from compositions at Mg/(Mg+Fe) ratios of 1.0, 0.85, 0.67, and 0.50. Temperatures along the series a_1, a_6, a_7, a_8 fall as follows 1278, 1262, 1240, 1210 °C.

The compositions studied at the Fe:FeO equilibrium were also studied with the oxygen pressure controlled at the Ni:NiO equilibrium, at which approximately 24% of the iron will be Fe^{3+}. In order to plot the diagrams, iron was recalculated as Fe^{2+}. The experimental data are plotted in figs. 3A to C which compared with figs. 1A to C show lower olivine but higher anorthite and augite liquidi. Temperatures are increased at this higher f_{O_2} as is shown by data in fig. 4A. Fig. 4B superimposes much of the data presented above.

In addition to the above data for compositions in the plane augite–anorthite–olivine, Humphries and Biggar (1981, fig. 51) published diagrams for a more siliceous join DI–L where L is $3CaO{\cdot}3Al_2O_3{\cdot}8MgO{\cdot}11SiO_2$ (figs. 5 and 8). These compositions contain normative hypersthene and intersect the anorthite–augite–olivine–liquid field boundary at points more siliceous than a_1, a_6, a_7, and a_8 and at lower temperatures. These points, designated b_6, b_7, and b_8 were found (Humphries

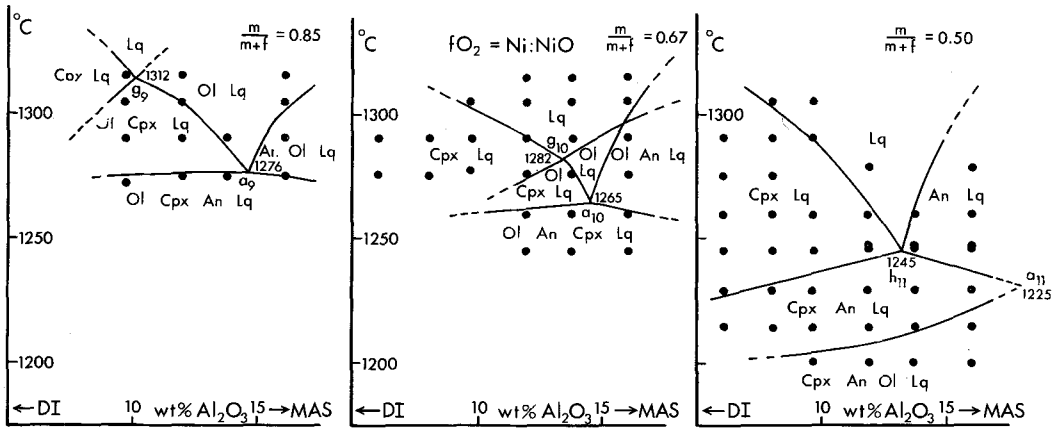

FIG. 3. Virtually as fig. 1 but f_{O_2} controlled at the Ni:NiO buffer.

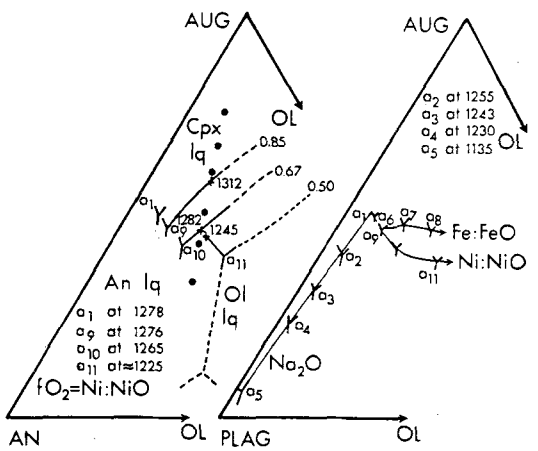

FIG. 4A (*left*). Information at several values of Mg/(Mg+Fe) superimposed, for experiments at f_{O_2} of Ni:NiO, data from fig 3. FIG. 4B (*right*). Composite derived from fig. 4A and fig. 2B and from Biggar and Humphries (1981) showing points at which the augite-plagioclase-olivine fields meet.

and Biggar, 1981, fig. 51) at 1260 °C, 1230 °C, and 1208 °C respectively. A summary of the phase relations of augite–plagioclase–olivine–liquid is presented in fig. 5 which records temperature variations against variations in Mg:Fe, Ca:Na, and pressure; it also records the variation of solubility of augite, plagioclase, and olivine with the same factors. These solubilities, in turn, control the proportions of the phases crystallizing, that is the composition of the equilibrium 'gabbro' extract, and hence the composition of the daughter 'residual' liquid.

We can deduce from fig. 5 that replacing MgO by FeO reduces the olivine field, lowers the temperature of first appearance of the plagioclase + augite + olivine, increases the normative olivine content of the liquids, but has little effect on the proportions of augite and plagioclase soluble in the liquid; that changing f_{O_2} does not alter these observations qualitatively; that replacing anorthite by albite rapidly shrinks the plagioclase field (soda-rich plagioclase is much more soluble in the liquids) but that temperatures decline slowly at least as far as replacement by $An_{33}Ab_{67}$ (Biggar and Humphries, 1981); and that increasing pressure reduces the augite solubility.

During normal classical differentiation of basaltic magmas, Fe/Mg increases, Na/Ca increases, and normative hypersthene or silica increase. These three factors all act in the same sense, of decreasing augite solubility, from which it would be expected that once augite starts to crystallize it will continue to do so. On the contrary, an ascending magma rising stepwise will, after each step, have to re-equilibrate to the phase relations appropriate to its new lower pressure at which there will be a decreased augite phase volume. Pressure drops therefore tend to leave, temporarily, a liquid undersaturated with augite which can only crystallize plagioclase or olivine or both for some interval before regaining the plagioclase–augite–olivine equilibrium. Such liquids probably actively resorb augite microphenocrysts and phenocrysts, and may be intruded and preserved in the geological column before regaining the cotectic, and reprecipitating augite.

Experimental remelting of oceanic tholeiites

Several authors have remelted samples of oceanic tholeiites in the laboratory at one atmosphere and

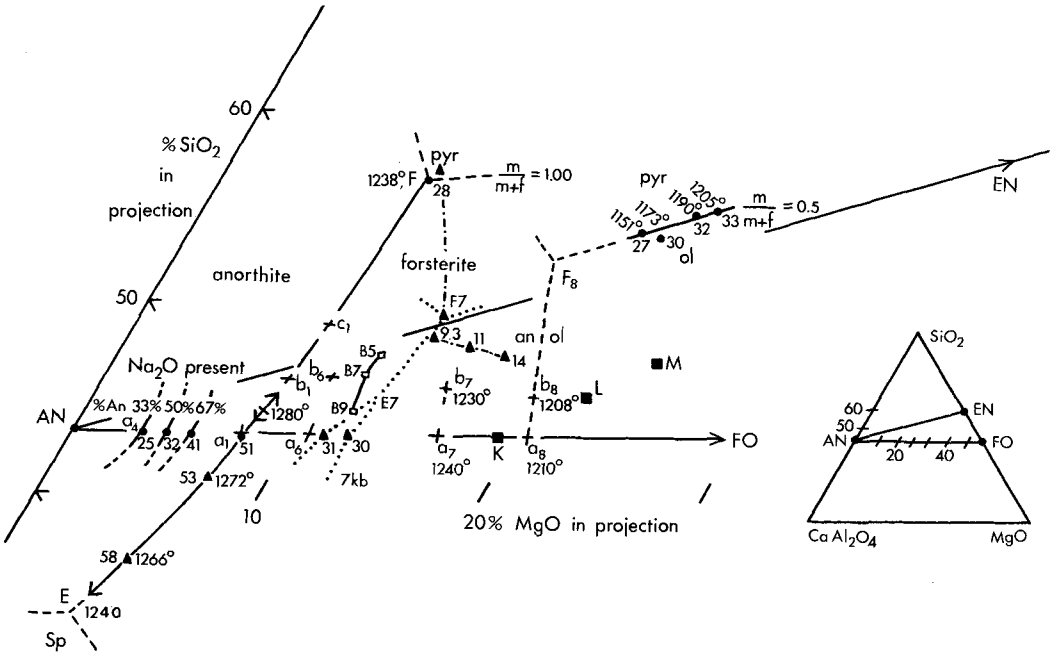

FIG. 5. Temperature and solubility data for the equilibrium plagioclase–augite–olivine–liquid, shown as a projection from diopside into An–Fo–SiO_2. The best documented curve for liquid compositions is that for CaO–MgO–Al_2O_3–SiO_2 at one bar which runs from the univariant points Di–Fo–En–Lq shown here as F at 1244 °C, up to a thermal maximum at a_1, and down to An–Di–Fo–Sp–Lq shown here as E at 1240 °C. The composition of F is known from Mori and Biggar (1981) and its temperature must be less than that of an experiment at 1246 °C using IPTS-68 (wrongly shown as 1240 °C in Mori and Biggar (1981)). The composition of E, shown using dashed lines, is in reality off the scale in this projection but its temperature is well documented at 1233.5 °C which converts to 1240 °C using IPTS-68. Data from Presnall *et al.* (1978, 1979) are shown as filled triangles. Data from Biggar and Humphries (1981) place the thermal maximum at > 1280 < 1286 °C between a_1 and b_1 and also record c_1 at > 1264 < 1278 °C.

Diopside solubility is expressed as a value between 0 and 100. 100 represents the diopside, or projection apex and 0 represents the plane An–Fo–SiO_2 which contains zero potential diopside. The diopside solubility falls from a maximum of about 60 at E to 51 at a_1, near the thermal maximum, to 28 at F. This fall from a_1 to F is clearly seen later in three dimensions in fig. 8.

As Na_2O replaces CaO the equivalent curves at 67, 50, and 33% An are displaced towards the AN apex, the augite solubility decreases from 51 to 25, and temperatures drop to > 1227 < 1234 °C at a_4 (Biggar and Humphries, 1981, fig. 5).

As FeO replaces MgO the equivalent curves are displaced towards FO, and a_6, a_7, a_8, are shown schematically (taken from fig. 1) along with b_6, b_7, b_8 from Humphries and Biggar (1981). Temperatures decrease, as shown, but the positions of these points in projection are only schematic since compositional data are not known. However, some microprobe compositional data for liquids along a different field boundary, olivine–pigeonite–augite, are known (Biggar, 1981) for samples with Mg/(Mg+Fe) = 0.5 from experiments made at the same time as those which yielded the point a_8 and the projected analyses at 1205, 1190, 1173, and 1151 °C are used to estimate the point F_8. The solubility of augite is little affected, as seen by the positions of a_1, a_6, a_7, and a_8 in fig. 2B.

As pressure increases the locus of F is, or is close to, the lherzolite solidus (Presnall *et al.*, 1979) shown as a dash dot line at 7, 9.3, 11, and 14 kbar. Also as pressure increases the temperature of the univariant E rapidly approaches the temperature of the thermal maximum (near a_1) and when E overtakes the thermal maximum the thermal divide is breached (the diopside plus spinel field crosses the plane DI–AN–FO. Anorthite and forsterite are no longer stable with liquid, for compositions in the plane, although they are still stable in more siliceous liquids between the points E7 and F7. At slightly higher pressures that stability vanishes when enstatite–spinel become stable with the liquids.

At 7 kbar diopside is less soluble (values about 30) compared with a value of 51 at 1 bar.

[Note added in proof: In fig. 5, for 1238°, F read 1244°, F]

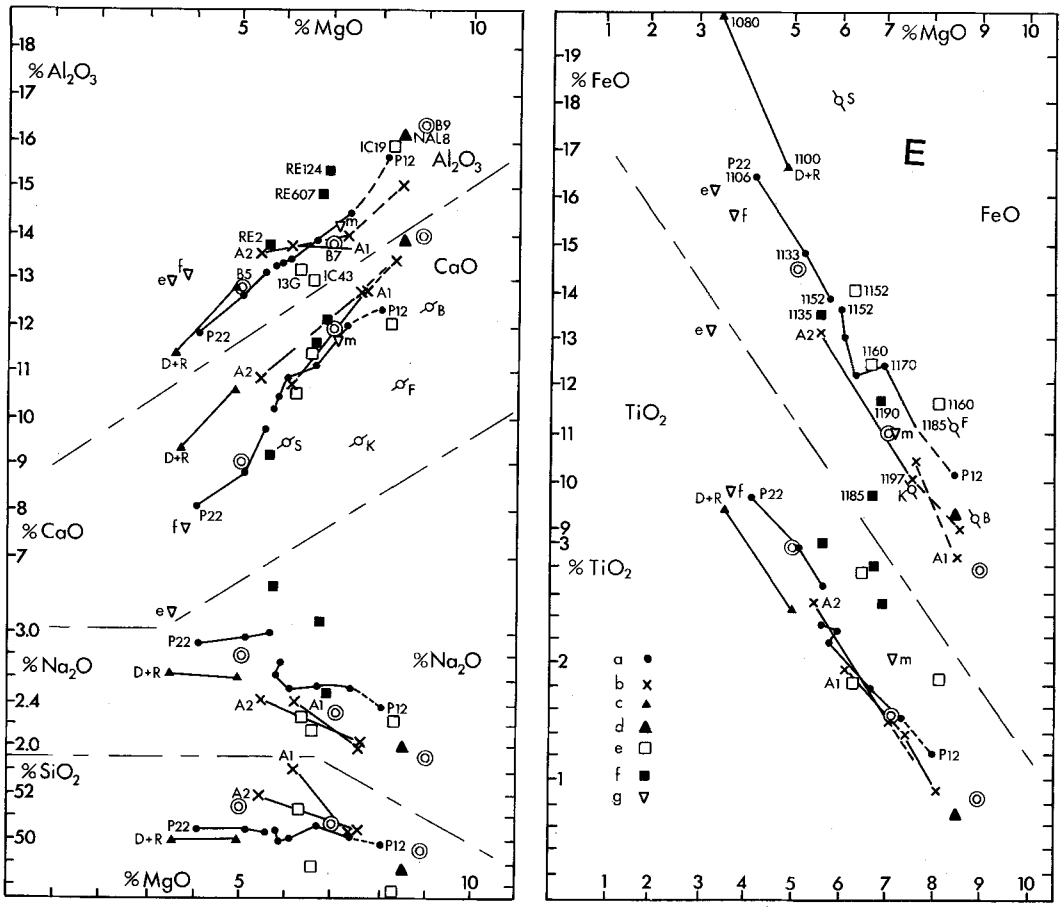

FIG. 6. Compositions of glasses from experimental charges of remelted ocean tholeiites, in equilibrium with plagioclase, augite, and olivine. The three double circles B5, B7, and B9 were interpolated to summarize the data and they appear in subsequent diagrams (also Table I).

The details of the data can be worked out from the sample numbers in the Al_2O_3 *vs.* MgO diagram and from the temperatures at which samples reach or remain in the equilibrium which are shown only in the FeO *vs.* MgO diagram. Details and symbols as follows: (*a*) Samples P12 and P22 from Walker *et al.* (1979) at QFM. These runs approached equilibrium except possibly for some of the pyroxene crystals for which K_D for the FeO : MgO ratio does not vary logically with temperatures. (*b*) Samples A1 and A2 from Biggar and Kadik (1981) at Ni : NiO. Some large non-equilibrated relicts (20 μm) of plagioclase and augite from the insufficiently ground up starting material survived the runs. (*c*) The line D + R from Dixon and Rutherford (1979) at molybdenum : molybdenum oxide. These cooling experiments are probably intermediate between equilibrium and fractional crystallization. Only data from (*a*) and (*b*) are used to select the points B5, B7, and B9. One whole rock analysis from Sigvaldason, 1974 (his sample NAL 8, large filled triangle, *d*), is inserted here to show that it is very much on the trend of liquid composition between B9 and B7, except for its lower TiO_2 content, and because it is used in later specimen calculations (fig. 11).

Other analyses from other suites of basalts (mainly from ocean island lavas which have higher levels of TiO_2) are plotted; (*e*) two remelted Icelandic basalts (higher TiO_2) and one basalt from Reykjanes ridge (lower TiO_2) at QFM from Fisk *et al.* (1980 and pers. comm.); (*f*) from Réunion, at or just above Ni : NiO (Humphries, 1975)—these are not probe analyses, but whole-rock analyses of samples which were observed to be cotectic; (*g*) these represent a model basalt (*m*) proposed by Cox (1980) and its calculated daughter liquid after equilibrium crystallization (*e*) and after fractional crystallization (*f*) but to keep the figure more simple the lines connecting the parent (*m*) to (*e*) and (*f*) are not shown but are almost parallel to the trend of experimental liquids. Items (*e*) to (*g*) suggest that cotectic liquids in other basaltic suites have very similar major element chemistry to the ocean tholeiites.

The effect of pressure is little known but on two of the diagrams (MgO *vs.* CaO and MgO *vs.* FeO) four points are shown, labelled B, F, K, S, for which see fig. 7.

at various oxygen fugacities. The observed crystallization sequences were olivine, plagioclase, augite; and plagioclase, olivine, augite (Walker *et al.*, 1979, and Biggar and Kadik, 1981). When olivine and or plagioclase crystallize there was much liquid present, but the appearance of augite marks a large increase in the proportion of crystals relative to liquid and a rapid decrease in the size of interstitial liquid pools with the risk that probe analyses of the quenched glasses become unrepresentative of the pre-quench equilibrium liquid due to quench effects. As a result few data exist for glasses in equilibrium with the three phases, augite, plagioclase, and olivine, and for any one sample such data cover a very limited temperature range as increasing solidification makes analyses impossible. The available liquid compositions in the equilibrium augite, plagioclase, olivine, liquid, are shown in fig. 6. To summarize these compositions for use in later diagrams and for the non-specialized reader, a trend based on three liquid compositions (Table I) was interpolated. For the

TABLE I. *Representative liquid composition in equilibrium with plagioclase-augite-olivine in experimental studies*

	SiO_2	Al_2O_3	TiO_2	FeO	MgO	CaO	Na_2O	K_2O
B9	49.5	16.5	0.8	8.0	9.0	14.0	1.9	0.15
B7	50.5	13.8	1.5	11.0	7.0	12.0	2.3	0.30
Cox	50.8	14.2	2.0	11.0	7.1	11.7	2.3	1.02
B5	51.5	12.8	3.0	14.5	5.0	9.0	2.8	0.60

specialist, the diagram shows what is known of cotectic liquid compositions in several basaltic suites. One of the three interpolated compositions is very close (apart from its K_2O and TiO_2 contents) to the model basalt composition proposed by Cox (1980) for continental flood basalts.

The effects of changing oxygen pressure at one bar total pressure are uncertain. The three representative compositions were selected using the data of Walker *et al.* (1979) at QFM and Biggar and Kadik (1981) at Ni:NiO. A few experiments by Biggar and Kadik at lower oxygen pressure were invalidated because Na_2O losses from samples held on wire hooks, at low oxygen pressure, can reach 50%. Humphries (1981) remelted a series of basalts from Réunion which have higher K_2O, TiO_2, and Na_2O than the ocean tholeiites. He used capsules of molybdenum, at low f_{O_2}, and AgPd alloys, at higher f_{O_2}, which almost eliminated soda loss although there was some iron loss at higher f_{O_2}. In general he found that the cotectic assemblage, plagioclase, augite, olivine, (often with spinel at higher f_{O_2}) was less stable by 5 to 25 °C at lower oxygen pressure. If this applies to tholeiites then the apparent discrepancy of lower temperatures of augite appearance found by Bender *et al.* (1978) is partially accounted for by the low f_{O_2} used by Bender. Such direct comparisons are uncertain because each investigator used an ocean tholeiite sample with slightly different chemistry.

Increase in total pressure causes the clinopyroxene field to expand, such that clinopyroxene becomes the liquidus phase, at the expense of the olivine and plagioclase fields (Fujii and Kushiro, 1977, Bender *et al.*, 1978). The apparent stability range of the assemblage is shown by four points in fig. 7 and some chemical data (MgO, FeO, and CaO which are plotted in fig. 6) demonstrate very small changes of liquid composition with pressure. The changes are even smaller for the other elements which are not plotted in fig. 6. From fig. 7 it seems that the low K_2O, low TiO_2 ocean tholeiites preserve the augite, plagioclase, olivine liquid assemblage to higher temperatures, at $7\frac{1}{2}$ to 10 kbar, than do the K_2O- and TiO_2-rich transitional or alkalic samples.

Liquids, crystal extracts, and major element trends in the crystallization of tholeiitic basalts

Natural examples. A tholeiitic liquid from which plagioclase, augite, and olivine are crystallizing will lie on one of a family of curves of the type *a*–F

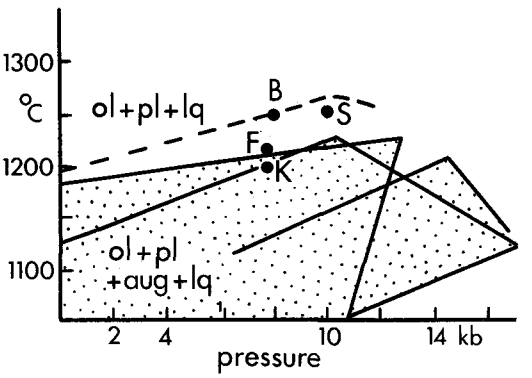

FIG. 7. The range of stability of the assemblage plagioclase-augite-olivine-liquid. The full lines and stippled areas are composite overlays for intermediate and alkalic basalt suites (Thompson 1974, Takahashi, 1980) which contain more K_2O, more TiO_2, and more Na_2O than mid-ocean basalts. The same assemblage is retained to higher temperatures by mid-ocean basalt samples, the data points being B from Bender *et al.* (1978); S from Stolper (1980); F from Fujii and Kushiro (1977); and K from Kushiro (1973) at which point Ca-poor pyroxene was also present. The dashed line suggests the apparent stability range for the assemblage in mid-ocean basalts.

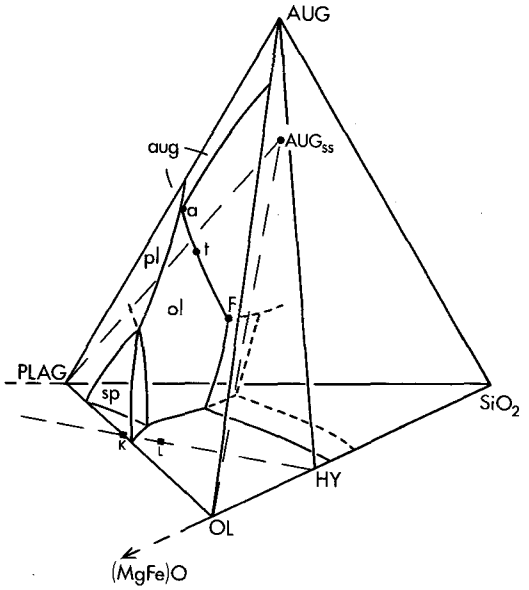

FIG. 8. The sub-system AUG–OL–PLAG–SiO_2, showing one position of the equilibrium plag–ol–aug–lq as the curve a_1–F. This curve intersects the plane defined by the actual compositions of the crystals, AUG_{ss}–PLAG–OL at *t*. Tangents to the curve will also intersect this plane, probably very close to *t*, and, in the limit when the curve is a straight line, actually, at *t*.

(fig. 8). The position of the curve within the tetrahedron will vary according to the Na_2O and FeO contents of the basalt and according to the total pressure. The composition of the plagioclase (with very minor FeO content) and the olivine (with very minor CaO content) can be considered as fixed, but the solubility of hypersthene and of alumina in augite may be large and is represented in fig. 8 by a point such as AUG_{ss}. The extract will lie on a plane such as AUG_{ss}–OL–PLAG. The instantaneous extract, (the precipitating crystals, for perfect fractional crystallization) will be where the tangent to the curve *a*–F intersects the plane AUG_{ss}–PLAG–OL. This point gives the proportions of the crystals in the extract.

Making the simplifying assumptions that the curves of the type *a*–F are nearly straight lines particularly near the *a* end and that the plane containing the extract is not very far removed from the liquid, means that the extract is very similar to its parent. An almost perfect demonstration of the truth of this is found in a study by Richardson (1979) of the Tandjiesberg Sill. The sill shows symmetrical flow concentration of plagioclase, augite and olivine phenocrysts. Richardson analysed, and point counted, three sections across the sill and concluded that the chilled margin and hence the magma was intruded carrying 23% of phenocrysts in the weight proportion, plagioclase 59, augite 26, olivine 15, and that the maximum concentration of phenocrysts near the centre was 50%. He then calculated the liquid composition, and in one example (his table 2) gave the calculated crystal extract. Thus we have the following data: (i) a calculated liquid composition; (ii) a magma composition, the chill, being liquid plus 23% crystals; (iii) a magma composition, rock MT21, being liquid plus 49.8% crystals; (iv) the extract (phenocrysts) composition relating (ii) and (iii). These compositions are shown in three diagrams. One projected from diopside into CA–M–S (fig. 9); one projected from SiO_2 into the plane plagioclase, augite, olivine (fig. 10); and as binary variation diagrams (figs. 11A to C). The four Tandjiesberg compositions in figs. 9 to 11 suggest that the curve *a*–F is nearly straight. A clear trend towards silica enrichment is seen in fig. 9, and confirmed by examination of the silica solubilities in fig. 10, and equally there is a trend towards lower diopside solubilities as expected for a curve of the type *a* to F. The field evidence from the Tandjiesberg Sill leaves no doubt that the samples are related as parent and cumulate.

More abundant in the literature are examples of two lavas from the same province, which are believed to be related by crystal fractionation,

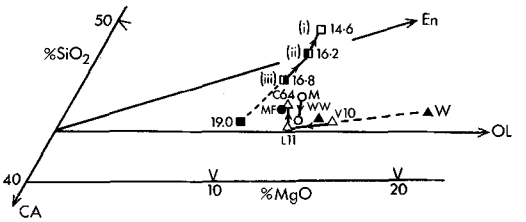

FIG. 9. Projection from diopside onto MgO–SiO_2–$CaAl_2O_4$ as in fig. 5. The Tandjiesberg data (shown as various square symbols with letters (i), (ii), and (iii) as defined in text) define a portion of a curve of the type *a*–F, connected by a dashed line to the crystal fractionate shown as a filled square. The figures beside the points, give the augite solubility of the points. There is a trend to lower augite solubility as expected for a curve of the type *a*–F (compare fig. 8).

Other examples in which a parent daughter relationship has been suggested for separate samples from the same province are shown as follows. Open circles for a parent, M, and daughter tholeiites, and a filled circle, MF, for the fractionate (Maaløe, 1979). Triangles (filled for the extracts) for data from Iceland from Wood (1978), using his sample numbers, V10 high magnesia basalt, L11 low magnesia basalt, C64 ferrobasalt, and W for his calculated extract going from high- to low-MgO basalt, and WW going from there to ferrobasalt.

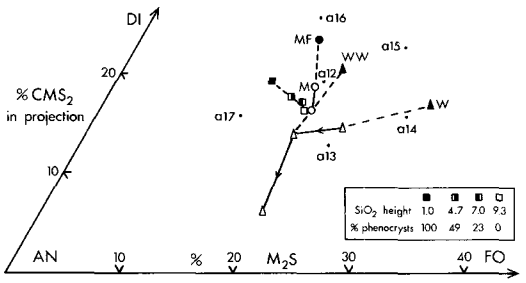

FIG. 10. Data for liquids and cumulates from fig. 9 recalculated with albite as its molar equivalent of anorthite, FeO equivalent to MgO, and projected from SiO_2 into Diopside–Anorthite–Forsterite. Symbols as in fig. 9. The inset shows, for the Tandjiesberg data, the percentage of phenocrysts in the samples and the 'SiO_2 height' which is a measure of the position of the samples, relative to the plane as zero and the projection apex (in this case SiO_2) as 100. The points a_{12} to a_{17} are discussed later in connection with fig. 12 and were calculated using An_{90}, Fo_{90}, and an augite as analysed by Walker *et al.* (1979). The natural liquids and extracts fall close to the compositions a_{12} and a_{13}, except for the rather olivine-rich first extract of Wood (1978). The Tandjiesberg data form a very close grouping.

although in the field this relationship cannot be proved. Two examples follow.

In the first example, Maaløe (1979) related two tholeiite compositions by a fractionate of 53% solids in the proportions plag $52\frac{1}{2}$, aug $40\frac{1}{2}$, olivine 7%. This fractionate when recalculated (figs. 9 and 10) and projected from SiO_2 into Plag–Aug–Ol appears in projection as the point MF. In this example the parent and the extract are even closer to each other than was the case for the Tandjiesberg Sill.

In the second example, for tholeiites from Eastern Iceland Wood (1978) chose a magnesian basalt (V10), a low magnesian basalt (L11), and a ferro-basalt (C64) and related the first two of these by extraction of 34% solids in the proportions 51% plag, 22% aug, 27% ol (his table 5) shown as W in figs. 9 and 10; and related the last two by extraction of 45% solids in the proportions 54.5% plag 36% aug 9.5% ol shown as WW in figs. 9 and 10.

The major-element chemical variation of Atlantic and Pacific ocean basalts was examined using binary variation diagrams by Flower (1980), and by Maaløe (1979). One of the trends was assigned to crystallization of plagioclase, augite, and olivine, and recognition of this trend, with various calculations of the proportions of the minerals involved, appear in le Roex *et al.* (1981) for samples from the FAMOUS area and in Staudigel and Bryan (1981) for samples from IPOD holes 417 and 418. Both papers recognize the control that cotectic crystallization of plagioclase–augite–olivine has on the evolution of the samples, and the latter in particular recognises that phenocryst redistribution during eruption and cooling is sufficient to

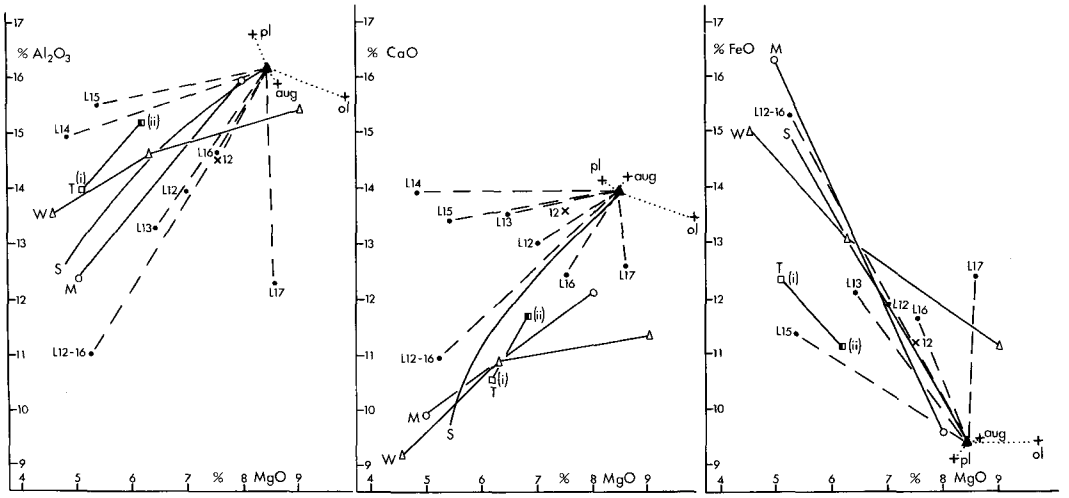

FIG. 11. Liquid evolution curves plotted as variation diagrams against MgO. Natural examples shown as full lines, T for Tandjiesberg, M for Maaløe, W for Wood, using symbols from fig. 10. The curved trend, S, has its origins and is discussed later in fig. 14 in connection with data from Iceland (Sigvaldason, 1974). Calculated trends are dashed lines which are discussed in the text. The trends start from the composition of a basalt, NAL8, shown as a filled triangle, as it was in fig. 6 in which it was also shown to lie on the trend of liquid compositions between B7 and B9. The plus signs represent the addition of 3.3 wt. % phenocrysts to NAL 8.

account for the within-hole variation in whole-rock analyses while also demonstrating that glass analyses (discussed later in fig. 18) are confined to a trend representing the liquid compositions in the cotectic.

Very similar major-element variation is known for continental flood basalts (Cox, 1980). The examples from above are shown in fig. 11, as variation diagrams, along with data from Iceland (Sigvaldason, 1974) which are discussed later (fig. 14). The trends are substantially parallel (except for the early part of the East Iceland trend (Wood, 1978) in which rather more olivine was needed in the crystal extract to get the best fit for mass balance) and are controlled by the proportions of plagioclase, augite, and olivine that crystallize, as will be demonstrated in the next section.

Calculated trends. The close resemblance of the parent, the extract, and the daughter was found to be sensitive to the proportions of the minerals crystallizing. To demonstrate this, some model calculations were made, and arbitrary, but reasonable, compostions of liquid and compositions of minerals had to be chosen (as Cox (1980) had to do for continental flood basalts).

The proportions of minerals in the extract chosen for the calculations are given by the points a_{12} to a_{17} in fig. 12. The starting liquid chosen was a basalt (described by Sigvaldason (1974) as sample NAL8) which is a K_2O-, TiO_2-, Zr-poor sample and which may be little evolved (see later discussion of Sigvaldason's data).

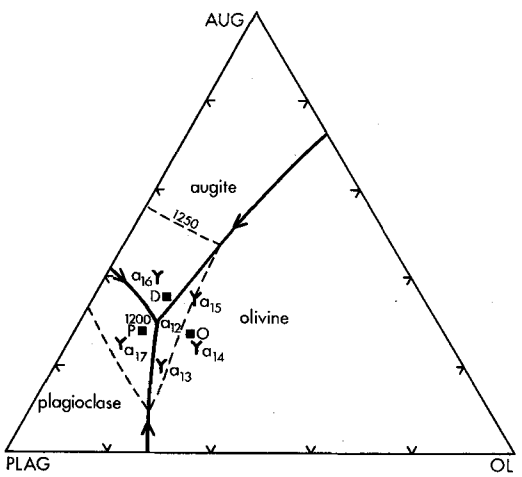

FIG. 12. The plane OL–AUG–PLAG with the expected form of phase diagrams estimated from Humphries (1975) showing the primary fields meeting at a_{12} (plag 55%, aug 30%, ol 15%). Addition of 10 wt. % phenocrysts to the composition a_{12} generates the points P when plagioclase is added, O when olivine is added, and D when augite is added. The points a_{13} to a_{17} represent other proportions of the primary phases and these proportions were used in model calculations shown in the last figure.

In the first instance the mineral extract was chosen to be plagioclase, An_{90}, olivine, Fo_{90}, but the choice of augite was more difficult. Trials with compositions such as Di_{64} En_{16} Hd_{16} Fs_4 were less satisfactory than with a real alumina-bearing augite and accordingly an augite from an experimental charge at 1185 °C (Walker *et. al.*, 1979) was chosen. Its composition, in weight percent, is SiO_2 48.6%, TiO_2 1.4, Al_2O_3 5.4, FeO 10.1, MgO 13.6, CaO 19.9, Na_2O 0.46. When crystals are extracted, such that 33.3% of the initial liquid solidified, in the proportions of a_{12} (given as plag 55, aug 30, ol 15 in fig. 12) then the residual liquid has the composition L12 (fig. 11) and likewise when the extract is a_{13} (plag 60, aug 20, ol 20) the residual liquid is L13 and so on for 14, 15, 16, 17.

Resemblance to the trend shown by the natural samples (fig. 11) is best shown by extraction of minerals in the proportion close to either a_{12} or a_{13} or a_{16} (fig. 11). Extracts based on a_{14} or a_{15} are too rich in olivine, leaving a MgO-poor liquid, and the a_{17} extract is so rich in plagioclase that the residual liquid contains more MgO than the initial liquid.

The above choice of minerals was arbitrary, but appropriate, for a basalt such as NAL8. If alternatively, Fo_{80} and An_{80} and the same augite are chosen, and the calculation reworked for a_{12} the resulting liquid is shown by a cross in fig. 11.

More complex two-stage calculations were made in which a further 33.3% of solids were extracted from the first batch of daughter liquids. One example using the proportions of a_{12} in the first batch and those of a_{16} in the second batch gave rise to the point L12–16 (fig. 11). Any number of such calculations are obviously possible, and various combinations of mineral compositions and mineral proportions will give better fits to any particular natural trend, but there is an obvious restriction in the proportion of the minerals that can be extracted. These proportions do not deviate much from the a_{16}, a_{12}, a_{13} region of fig. 12 and as much as 33% of a magma can precipitate, whilst the MgO (and some other major elements) only change by about 1% absolute (fig. 11). In summary, the arguments given in connection with figs. 9, 10, and 11, suggest narrow limits to the proportions of plagioclase, augite, and olivine which can precipitate and preserve the trend of basaltic compositions (see also Cox, 1980, and Maaløe, 1979). In the literature a much greater range of mineral proportions has been suggested by various authors for various suites of rocks particularly when trace

element data were used to calculate the proportions of these phases in the extract. Many of these mineral proportions are untenable with respect to major-element behaviour because they do not preserve basaltic chemistry, nor would they preserve basaltic mineralogy.

Phenocryst accumulation. The effects of phenocryst accumulation are examined in figs. 11 and 12, but note that in fig. 11 the crosses represent addition of 3.3 wt. % phenocrysts to the Icelandic basalt NAL8, and in fig. 12, the filled squares represent addition of 10 wt. % phenocrysts to a liquid a_{12}.

The nature of the liquidus contours on planes of the type plagioclase–augite–olivine is shown in fig. 12 to illustrate that the addition of the same wt. % of different phenocrysts to a chosen starting composition has unequal effects on liquidus temperatures. Thus, four samples are shown; the original liquid is shown at the plagioclase–augite–olivine field boundary position a_{12}, and the other three compositions are generated by adding 10 wt. % phenocrysts. In the hands, or crucibles, of the experimental petrologist, compositions P and D, enriched respectively in plagioclase and augite would show nearly cotectic behaviour, crystallizing feldspar or augite for only 12 °C before crystallizing the cotectic assemblage, but composition O would crystallize olivine for perhaps 60 °C before becoming cotectic, a behaviour, which might be less readily interpreted as that of a liquid close to the cotectic.

The effect on major element chemistry of even minor phenocryst accumulation can be significant. As little as $2\frac{1}{2}$% of olivine phenocryst changes MgO by 1% absolute. The chemistry of MgO in basalt is such that extraction of 1.8% olivine as phenocrysts changes the absolute MgO content by the same amount as 33.3% of cotectic crystal extraction of augite, plagioclase and olivine. This is re-emphasised, using an example shown in fig. 13A which shows for a given magma that there is a large 'cross-trend' effect produced by small accumulations of olivine or plagioclase but only a small 'down-trend' effect due to extensive cotectic crystallization as follows. If basalt P is an early composition of the magma batch then let it have *n* ppm of an incompatible element. Crystallization to the point L_{50} involves $2\frac{1}{2}$% olivine phenocrysts followed by 50% of cotectic crystallization. Subsequent eruption with pressure release, and accumulation of say $2\frac{1}{2}$% of new olivine phenocrysts will give compositions such as R. P and R may at first glance be considered as equally parental since they will both crystallize olivine first over a wide temperature range (refer to fig. 12). R has two times the trace element content of P which may suggest that it has been derived by lesser degrees of partial melting or derived from a portion of a heterogeneous mantle with more trace elements than the portion of a mantle from which P came. Likewise liquid L_{25} (fig. 13A) has four times the incompatible element content of P.

Re-examination of some previous data

The above noted chemical effects of phenocryst accumulation and of extensive cotectic crystallization warrant a reassessment of some recent studies of basalt petrogenesis. This re-examination

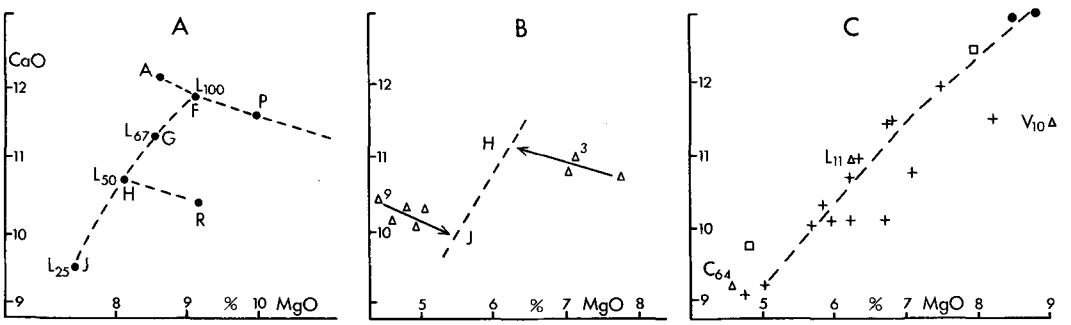

FIG. 13A. CaO *vs.* MgO variation diagram to illustrate the large effect of small amounts of phenocrysts and the small effect of large amounts of cotectic crystallization. L_{100} is an arbitrary basaltic liquid, P is the same enriched by $2\frac{1}{2}$% of Fo_{90} and A represents enrichment by $2\frac{1}{2}$% of An_{90}. L_{67}, L_{50}, and L_{25} represent derivative liquids after removal of 33, 50, and 75% of solids (plagioclase, augite, olivine). R is L_{50} with $2\frac{1}{2}$% olivine phenocrysts added. B. Data from Saunders and Tarney (1979) reinterpreted as an example of extensive fractional crystallization, between liquids H and J. Data are for dredge 24, Scotia back-arc (Saunders and Tarney, 1979). C. Samples from Sigurdsson *et al.* (1978) recorded as containing phenocrysts of augite, olivine, plagioclase. Two filled circles from Langjökull zone, and the crosses from Skagi. The dashed line is a suggested locus of liquids. Triangles from Wood (1978), see text. Open squares from Clague and Bunch (1976), see text.

shows that the data for particular suites of tholeiites can result from crystal fractionation, even in cases where the original author postulated a model of variable partial melting. Detection of the earliest co-precipitation of a magnesian olivine, a magnesian augite, and a calcic plagioclase, suggests samples which are possible parents for the rest of a suite.

The first example chosen is a suite dredged from the East Scotia back-arc (Saunders and Tarney, 1979) which is plotted in fig. 13B, and for which these authors proposed variable degrees of partial melting as the origin of the two groups of samples. The lines, arrows, and the symbols H and J are added to suggest that the basalts are analogous to H and J in fig. 13A. Sample 9 is reported as having phenocrysts (plagioclase 8.5%, olivine 1.4%) and sample 3 (olivine 3.5%, plagioclase 1.4%, augite 0.9%), and the arrows indicate my estimates of where the phenocryst-free liquids may be and the dashed line of how these liquids may be cotectic (by analogy with fig. 13A). This interpretation is consistent with 50% crystallization from H to J which explains the higher Zr, Ti, and Fe/Mg ratio in the plagioclase phyric basalts.

Fig. 13B also serves to illustrate that linear least squares calculations which try to relate phenocrystic samples such as sample 3 and sample 9 will fail to provide a sensible result if the crystallization-accumulation path follows a locus such as 3-H-J-9. Saunders and Tarney found 'negative plagioclase' using their assumptions about primitive and evolved liquids.

The second samples are from Iceland (Sigurdsson *et. al.*, 1978). Those of their samples which contained phenocrysts of augite, plagioclase, and olivine (plus spinel in some cases) are plotted in fig. 13C. By analogy with fig. 13A, the low MgO end could represent $87\frac{1}{2}$% crystallization from the high MgO end. Sigurdsson *et al.*, 1978 (p. 3977) comment that there is a limited degree of chemical dispersion within the Skagi group which they believe to indicate either a very minor extent of fractional crystallization or that the lavas have by chance all suffered a similar amount of fractionation. They further comment that this perplexes them in view of the evolved (TiO_2, P_2O_5, K_2O) nature of the Skagi group. An interpretation offered here, based on Figs. 9 to 11, suggests that the reverse is almost certainly true, and that their small chemical variations are down-trend ones which represent enormous amounts of crystallization, to give TiO_2, P_2O_5, K_2O enrichment. What remains perplexing is that they conclude, from a least squares fit, that less than 20% fractional crystallization covers their major element dispersion. This is in stark contrast to the broadly similar points V10, L11, C64, shown in fig. 13C for which Wood (1978) calculates 70% crystallization from V10 to C64, and to the two open squares for which a similar value, of 74% crystallization was calculated (Clague and Bunch, 1976).

Further examples from Iceland were published by Sigvaldason (1969) with analyses and a brief petrography of thirty-four basalts. He suggested that the tholeiites could be grouped into batches with slightly different primitive chemistry but *identical differentiation trends.* By contrast Sigvaldason in 1974 published analyses of thirty-six basalts from the northern part of the eastern volcanic zone in Iceland and suggested (p. 530) overlapping zones with *variable degrees of partial melting* as sources for these basalts. More in sympathy with the present work Wood (1978) analysed 130 lavas from Iceland and demonstrated that fractional crystallization could relate all his samples to each other and examples of his liquids and extracts have been discussed above in figs. 9, 10, 11, and 13C. Sigvaldason's (1974) data require reinterpretation. His thirty-six basalts belong to a continuous differentiated series but an arbitrary division into five stages along the series, is made here to aid discussion. The division is based on the groups marked A to E in the TiO_2 versus MgO variation diagram (fig. 14E). The groups D and E are poorly represented in Sigvaldason (1974) but are well represented in Sigvaldason (1969). For his 1974 series Sigvaldason selected three groups. I have split his first group into my groups A and B, except that I have included one extra sample (No. 33) indicated by the triangle with spikes. [This sample is clearly a member of group A in all respects except its K_2O content (Sigvaldason reports 0.26% K_2O whereas the rest of group A has close to 0.06% K_2O.] His second group corresponds with my group C, except that I have added two samples, shown as symbols with spikes. My groups C and D form a continuum rather than groups, but group D closely matches Sigvaldason's third group. The groupings A to D (allowing that the C to D boundary is diffuse) have a marginally greater success at grouping like with like (compare Sigvaldason's other trace element data and fig. 14F), than did Sigvaldason's groups.

Within each group one can interpret some samples as liquid compositions, and other samples being these same liquids with olivine and/or plagioclase accumulation and in figs. 14B, C, and E, the dashed lines are the suggested lines of evolution which a liquid precipitating, olivine, augite, and plagioclase would follow. The plus signs indicate the expected effects of accumulating olivine or plagioclase into these liquids (compare fig. 11). That this interpretation of the samples is reasonable

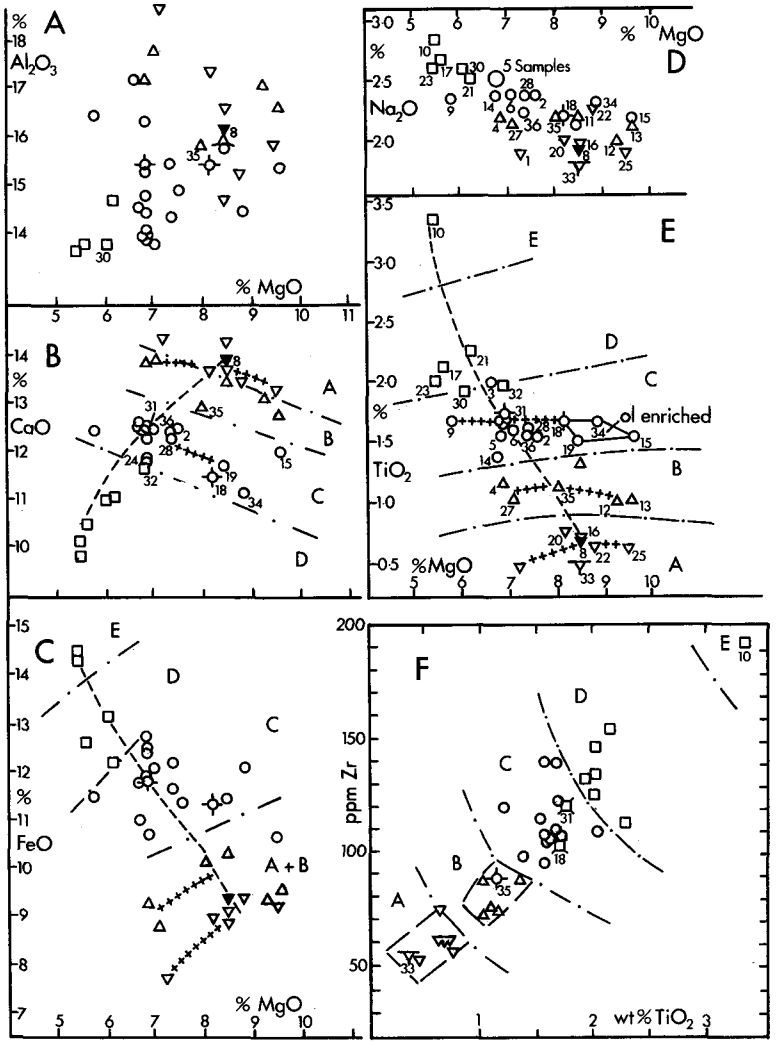

FIG. 14A to E. Variation diagrams for basalts from Iceland (Sigvaldason 1974). Numbers are his sample numbers and include NAL 8 which is specially identified as a filled triangle because it was used in fig. 11, as typical of group A. The five groups are defined on the basis of fig. E and are separated by dash dot lines, but a continuum probably exists in nature. The dashed line, in some figures, is a suggested trend for liquids in equilibrium with plagioclase, olivine, augite. Lines composed of plus signs indicate samples interpreted as olivine or plagioclase cumulates into liquids lying on the dashed lines. F is a redrawn version of Sigvaldason's fig. 7 in which symbols with spikes are shown to belong to groups other than the group to which Sigvaldason assigned them, and No. 33, omitted by Sigvaldason is drawn in. Thus No. 35 belongs to group B, not C, and 18 and 31 to group C, not D, and these changes are supported by most of the trace element data reported in Sigvaldason's tables.

can be confirmed by looking at the samples, in projection from diopside into CA-M-S (fig. 15). Samples which were to the right of the dashed line in fig. 14E and were presumed to have cumulus olivine, plot as groups in fig. 15, at a lower diopside height because of the cumulus olivine. Likewise, samples to the left were presumed to be plagioclase enriched and plot towards plagioclase at lower diopside heights. Samples close to the dashed lines, may be liquids in equilibrium with augite-plagioclase-olivine, and accordingly plot at a higher diopside height. The central portion of the diagram contains the liquids belonging to, groups A and B combined, group C, and group D, the

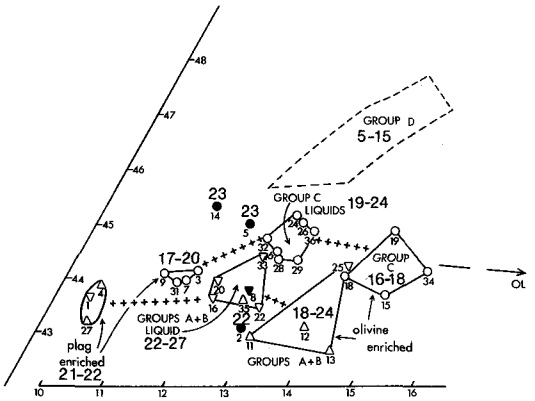

FIG. 15. Samples from fig. 14, Sigvaldason (1974) with his sample numbers below the points projected from diopside into CA–M–S (compare figs. 6 and 9). Larger numbers represent heights above the projection plane. Groups A and B are combined (as Sigvaldason did). Sample numbers allow comparison with fig. 14E and for example the samples 15, 18, 19, and 34, identified in fig. 14E as olivine enriched are identified above as a group, lying between samples identified as group C liquids and the olivine apex, and therefore lying at lower heights consistent with this accumulation of olivine.

field for this latter as shown in fig. 15 is drawn to encompass data from Sigvaldason (1969) which are not separately plotted in this paper. It is also possible for samples to be phenocrystic or cumulitic with any combination of two or three from augite + plagioclase + olivine, and samples believed to be of this type are shown by filled symbols. Wood (1978) emphasised that polymineralic accumulation produces, sometimes subtle and sometimes significant, effects on the chemistry of lavas, and not suprisingly a few of Sigvaldason's analyses do not fit the groupings given above. The central zone, containing the liquid compositions, (fig. 15) shows falling diopside heights from A to D and represents a curve of the type *a*–F (fig. 8). The basalt NAL8, at the MgO-rich end of the range of liquid compositions, for example in the CaO versus MgO diagrams (fig. 14B), was selected as representing a possible parent to the other basalts, and has been used already in connection with the extract calculations plotted in fig. 11. This sample is not special but just typical of group A basalts which are low TiO_2 < 0.8%, low Zr < 72 ppm, low Sr < 105 ppm, low K_2O < 0.09% (if the K_2O analysis of sample 33 is accepted as an error) and low FeO < 9.4%.

Group E basalts are iron- and titanium-rich and are not shown in fig. 15. They plot at very low diopside solubilities below the group A, B, and C liquids. Minor phases, magnetite, ilmenite, apatite (see Wood, 1978) have complicated the evolution of the liquids and the relatively simple model used in this paper, involving augite, plagioclase, olivine, and trends of the type *a*–F, is no longer appropriate for these group E basalts.

In the earlier paper (Sigvaldason, 1969) there are some petrographic descriptions which if read with the variation diagrams, and with the projections, confirm that small accumulations of olivine or plagioclase displace the chemical analyses as above. There was a larger number of more-evolved basalts in the 1969 study and these show three or fourfold increases in K_2O, TiO_2, and Zr with progressively less change in Na_2O, CaO, Al_2O_3. The basalts of groups A, B, C, and probably D can be linked by crystallization. We must not assume that group A basalts are themselves partial melts. Since they are in equilibrium with augite–plagioclase–olivine it seems probable that they too have crystallized these three phases, and there is no compelling reason to accept them as derived from crystallization or melting of some other equilibrium. Icelandic basalts fit the cotectic crystallization model in contrast to Sigvaldason's interpretation of each of his groups as a partial melt of mantle material, at different depth.

As a final illustration of the principles behind the reinterpretations of chemical, and modal data, another series of basalts from Iceland with petrographic descriptions and with modal analyses of phenocrysts, published by Jakobsson *et al.* (1978), is re-examined.

Jakobsson *et al.* (1978) distinguish two suites; an olivine–tholeiite suite from shield volcanoes (circles in fig. 16) and a tholeiite suite from fissure eruptions (squares). Arrows in fig. 16, represent subtraction of the phenocrysts present and lead to the dashed

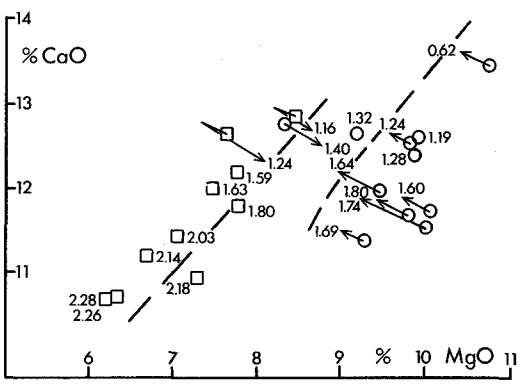

FIG. 16. CaO *vs.* MgO for olivine tholeiites from shield volcanoes (circles) and tholeiites from fissure eruptions (squares) from Jakobsson *et al.* (1978). Values are wt. % TiO_2.

lines which suggest loci of liquids. These loci suggest 50 to 75% of crystallization of augite, plagioclase, olivine (in each of these suites) and weight per cent TiO_2 values increase by factors of two or three, down the cotectic trend, for relatively small changes of about 2 wt. % absolute in MgO.

Diagrams of a very different type are employed by some geochemists to argue for an origin of the range of ocean basalts from partial melting processes. One example involving CaO/TiO_2 and Al_2O_3/TiO_2 ratios *vs.* wt. % TiO_2 from Sun *et al.* (1979) is shown in fig. 17, with data added for the basalts NAL8, NAL35, and NAL31, from fig. 14 to represent the suggested locus of liquids crystallizing augite, plagioclase, and olivine. Also added are the points L12 and L12–16 from the extract calculations (fig. 11). (These calculations used a particular augite with 1.4% TiO_2, but extraction of an augite containing a little less TiO_2 would make the L12 and L12–16 points in fig. 18 lie along the trends shown by Sun *et al.*, (1979).) The CaO/TiO_2 *vs.* TiO_2 and Al_2O_3/TiO_2 *vs.* TiO_2 trends of Sun *et al.* (1979) are just those expected for crystal fractionation models involving extraction of augite, plagioclase, and olivine in the proportions demanded by the phase equilibrium data. It is not clear from Sun *et al.* (1979) what material they are partially melting and they quote no calculation of liquids and residues.

Summary and discussion

Reinterpretation of other's data can not be entirely successful, but the combination of simple plots (fig. 14) and of complex projections (fig. 15), along with modal data for phenocryst contents can identify, and thereafter allow for, samples containing redistributed phenocrysts and thence one can deduce liquid compositions. Only these need be tested to prove that they are related by co-precipitation in the proportions demanded by the phase relations. A selection of such deduced liquid compositions is shown in fig. 18 but first the variation, or inhomogeneity, which can arise in a single lava flow, recently investigated by Lindstrom and Haskin (1981), results in short range (several centimetres) segregation which can be as large as interflow compositional differences, and is certainly larger than analytical differences. The field surrounded by short dashed lines in fig. 18 contains the Lindstrom and Haskin data and is some measure of the variation which perhaps exists within the other suites which are nevertheless shown as simple curves.

The simple curves are the present author's visual assessment of where the liquids might lie, based on the published analytical and modal data, treated as described in fig. 13. The curve HJ, represents East Scotia samples from fig. 13B; LS, Icelandic samples from fig. 13C; S, Icelandic samples from fig. 14; JJS, Reykjanes samples from fig. 16; KS, samples from Kap Stosch (Noe-Nygaard and Pedersen, 1974) not separately illustrated in this paper; and the curve EXP is based on the experimental data (Table I and fig. 6).

Mid-ocean ridge samples are variously represented. The area defined by triangles shows the within-hole variation of glasses in IPOD holes 417 and 418 from Staudigel and Bryan (1981). The dotted area represents mid-ocean samples from Hekinian and Aumento (1973), the crosses being samples from the Gibbs fracture zone with higher TiO_2 contents, which samples are rather rare in the mid-oceans. Within this dotted area, but not shown individually, are plagioclase basalts, augite-phyric basalts, and aphyric basalts from ocean ridges. Other data for ocean basalts are from Morel and Hekinian (1980) who succeed in defining two trends (OS for oversaturated, and S for saturated) which must pass through the asterisks and which they distinguish from each other, apparently on a finer scale than Lindstrom and Haskin (1981) found within one flow.

If all the above is accepted as defining the major element chemistry, then the trend is due to cotectic differentiation, in which extensive crystallization builds up incompatible element concentrations (fig. 13B) even in this simple model. More complex processes in a magma chamber, as envisaged by O'Hara and Mathews (1981), lead to very much greater concentration of incompatible elements.

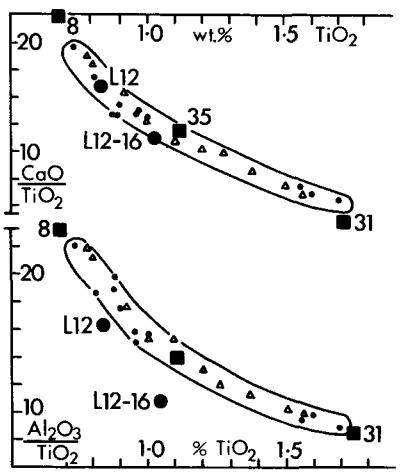

FIG. 17. Based on fig. 1 of Sun *et al.* (1979) with various superimposed points from figs. 11 and 14 of this paper.

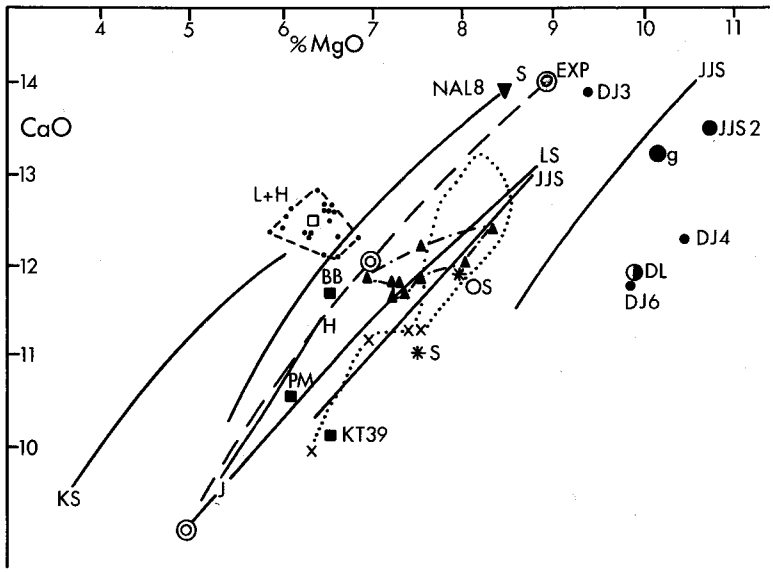

FIG. 18. Liquid compositions in equilibrium with plagioclase, augite, and olivine, summarised as curves and areas. Circular symbols are calcic, and often aphyric dykes from tholeiitic provinces. DJ from Drever and Johnstone (1966), JJS 2 from Iceland (Jakobsson *et al.*, (1978) see fig. 16 of this paper). Also shown is a point DL, from Irvine (1977) chosen by him as a derivative liquid from abyssal tholeiites. It is actually the average of some olivine-phyric basalts from DSDP Leg 37, and olivine must be subtracted from it to give the liquid composition. *g* quoted from Wood (1978) is one of the most magnesian ocean-basalt glasses known (from DSDP Leg 3). Most of the data represented by circular symbols approach, or after crystallization of 5 or 10% olivine would approach, the calcic ends of the loci of liquids which crystallize augite, plagioclase, and olivine. Chilled margins of tholeiitic bodies are shown as filled squares, BB for Ben Buie and PM for a Preshal Mhor Dyke, both quoted from Skelhorn *et al.* (1979) and KT39 for a 'new' Skaergaard liquid from Hoover (1978).

Such a magma chamber may be 'sampled' when liquid is ejected (one assumes to lower pressure, such that plagioclase and olivine phenocrysts will grow, and augite nucleii, and even phenocrysts, will dissolve), cooled, and preserved in the geological record. Cotectic evolution in a quiescent period leaves only gabbroic cumulates, and liquid is not preserved in the geological record until the next ejection. Thus successively ejected liquids carry the chemical evidence of cotectic crystallization of augite, plagioclase, and a little olivine despite their modal phenocryst contents which generally lack augite. The high Ca end of the trend corresponds to various calcic, aphyric dykes, which are also

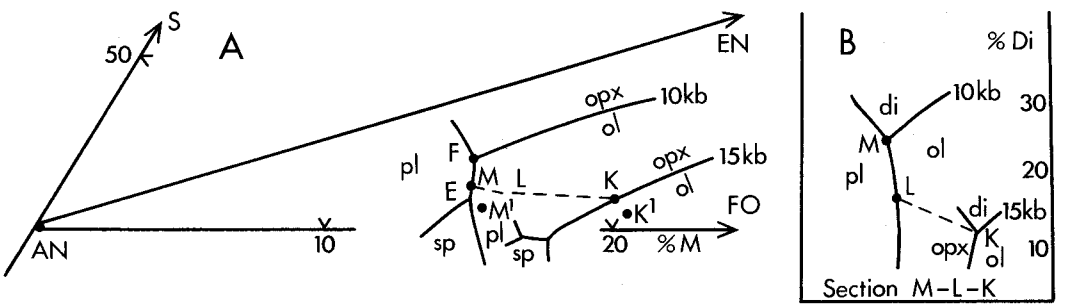

FIG. 19. Projection from diopside into CA–M–S. The curve at 15 kbar based on Stolper (1980) represents liquids in equilibrium with augite + olivine + orthopyroxene and is one of an infinite family, each value of MgO/(MgO + FeO) and Na/(Na + Ca), etc. giving rise to a slightly different curve such as the one that may be imagined to pass through K^1. If the liquid at K is brought to 10 kbar it will crystallize olivine to L, then olivine and plagioclase to M, as shown in fig. A. The pseudo-section (fig. B) shows the relative augite saturation levels of the points K, L, and M.

low-K_2O, low-TiO_2, low-trace element compositions and examples are detailed in the caption to fig. 18. By contrast, the chilled margins of tholeiitic intrusions plot well down the differentiation trend. The assemblage augite, plagioclase, olivine, liquid, ceases to be stable at about 10 kbar, but as yet there are no experimental data to determine how this varies with changing olivine, feldspar, and augite compositions, nor to determine if the range of calcic compositions in fig. 18 represents a range of liquids formed at different pressures, or formed from different Mg/(Mg + Fe) or Ca/(Ca + Na) sources. All such liquids could be partial melts of a pre-existing plagioclase peridotite, or similar, see Stolper *et al.* (1979) but, on Earth, are much more probably derived from a mantle source which left behind residual olivine, orthopyroxene, and perhaps augite as for example, liquid K in fig. 19, which if brought to 10 kbar would crystallize olivine, to the point L, then olivine and plagioclase between L and M. Other liquids such as K^1, derived from perhaps a different temperature, pressure, or Mg/Fe regime, will attain a different point M^1, on a different 10 kbar curve. There are no data to quantify these effects for compositions in the system CaO–Na_2O–FeO–MgO–Al_2O_3–SiO_2 and very limited data for remelted rocks.

Acknowledgements. Much of the inspiration behind the first section of the paper derives from work jointly done with D. J. Humphries. Many colleagues have helped to improve the text and encouraged me to rewrite it, including David F. Strong, Martin Fisk, and Colin H. Donaldson.

REFERENCES

Bender, J. F., Hodges, F. N., and Bence, A. E. (1978) *Earth Planet. Sci. Lett.* **41,** 277–302.
Biggar, G. M. (1981) *Bull. Mineral.* **104,** 375–80.
—— and Humphries, D. J. (1981) *Mineral. Mag.* **44,** 309–14.
—— and Kadik, A. (1981) *Progr. Exptl. Petrol.* **5,** 122–6.
Clague, D. A., and Bunch, T. E. (1976) *J. Geophys. Res.* **81,** 4247–56.
Cox, K. G. (1980) *J. Petrol.* **21,** 629–50.
—— Bell, J. D., and Pankhurst, R. J. (1979) *The interpretation of igneous rocks.* George Allen & Unwin, London. 450 pp.
Dixon, S., and Rutherford, M. J. (1979) *Earth Planet. Sci. Lett.* **45,** 45–60.
Drever, H. I., and Johnstone, R. (1966) *J. Petrol.* **7,** 414–20.
Fisk, M. R., Schilling, J. G., and Sigurdsson, H. (1980) *Contrib. Mineral. Petrol.* **74,** 361–74.
Flower, M. F. J. (1980) Nature, **287,** 530–2.
Fujii, T., and Kushiro, I. (1977) *Carnegie Inst. Wash. Yearb.* **76,** 461–4.
Hekinian, R., and Aumento, F. (1973) *Marine Geol.* **14,** 47–72.
Hoover, J. D. (1978) *Carnegie Inst. Wash. Yearb.* **77,** 739–43.
Humphries, D. J. (1975) *Phase Equilibrium studies of some basalt-like compositions in the system* CaO–MgO–Al_2O_3–SiO_2–Na_2O–Fe–O_2. Thesis Edinburgh University.
——(1981) *Progr. Exptl. Petrol.* **5,** 133–4.
—— and Biggar, G. M. (1981) Ibid. **5,** 148–60.
Irvine, T. N. (1977) *Carnegie Inst. Wash. Yearb.* **76,** 454–61.
Jakobsson, S. P., Jonsson, J., and Shido, F. (1978) *J. Petrol.* **19,** 669–705.
Kushiro, I. (1973) *Tectonophys.* **17,** 211–22.
le Roex, A. P., Erlank, A. J., and Needham, H. D. (1981) *Contrib. Mineral. Petrol.* **77,** 24–37.
Lindstrom, M. M., and Haskin, L. A. (1981) *Geochem. Cosmochim. Acta,* **45,** 15–31.
Maaløe, S. (1979) *Lithos,* **12,** 59–72.
Morel, J. M., and Hekinian, R. (1980) *Contrib. Mineral. Petrol.* **72,** 425–36.
Mori, T., and Biggar, G. M. (1981) *Prog. Exptl. Petrol.* **5,** 144–5, 147.
Noe-Nygaard, A., and Pedersen, A. K. (1974) *Bull. Geol. Soc. Denmark* **23,** 175–90.
O'Hara, M. J. (1976) *Prog. Exptl. Petrol.* **3,** 103–26.
—— and Matthews, R. E. (1981) *J. Geol. Soc.* **138,** 237–77.
Presnall, D. C., Dixon, J. R., O'Donnell, T. H., Brenner, N. L., Schrock, R. L., and Dycus, D. W. (1978) *Contrib. Mineral. Petrol.* **66,** 1232–41.
———— and Dixon, S. A. (1979) *J. Petrol.* **20,** 3–35.
Richardson, S. H. (1979) *Geochim. Cosmochim. Acta,* **43,** 1433–41.
Saunders, A. D., and Tarney, J. (1979) Ibid. **43,** 555–72.
Sigurdsson, H., Schilling, J-G., and Meyer, P. S. (1978) *J. Geophys. Res.* **83,** 3971–82.
Sigvaldason, G. E. (1969) *Contrib. Mineral. Petrol.* **20,** 357–70.
——(1974) *J. Petrol.* **15,** 497–524.
Skelhorn, R. R., Henderson, P., Walsh, J. N., and Longland, P. J. N. (1979) *Scott. J. Geol.* **15,** 161–7.
Staudigel, H., and Bryan, W. B. (1981) *Contrib. Mineral. Petrol.* **78,** 225–62.
Stolper, E. (1980) Ibid. **74,** 13–27.
—— McSween, H. Y., and Hays, J. F. (1979) *Geochim. Cosmochim. Acta,* **43,** 589–602.
Sun, S-S., Nesbitt, R. W., and Sharaskin, A. Y. (1979) *Earth Planet. Sci. Lett.* **44,** 119–38.
Takahashi, E. (1980) *Carnegie Inst. Wash. Yearb.* **79,** 271–6.
Thompson, R. N. (1974) *Contrib. Mineral. Petrol.* **45,** 317–41.
Walker, D., Shibata, T., and De Long, S. E. (1979) Ibid. **70,** 111–25.
Wood, D. A. (1978) *J. Petrol.* **19,** 393–436.

[*Manuscript received 22 February 1982; revised 15 July 1982*]